94-GT-381

EFFECT OF INCIDENCE ON SECONDARY FLOWS
IN A LINEAR TURBINE CASCADE

G. V. Ramana Murty
Turbomachinery Laboratory
Corporate Research and Development
Bharat Heavy Electricals Limited
Hyderabad, India

N. Venkatrayulu
Thermal Turbomachines Laboratory
Indian Institute of Technology
Madras, India

ABSTRACT

The effect of incidence on the generation and growth of secondary flows in a linear turbine cascade was studied in the present investigations using a Variable Density Cascade Tunnel at an exit Mach number of 0.49 and a Reynolds number of 8×10^5. The angles of incidence chosen were $+15^0$, $+5^0$, 0^0, -5^0 and -8.5^0. The flow field was surveyed at five axial stations from cascade inlet to exit with a view to understanding the development of the secondary flow with the help of the variation of mass averaged total pressure loss coefficient and the contours of local loss coefficients in the pitch and spanwise directions. The total pressure loss coefficient and the net secondary loss coefficient have shown a steady growth along the cascade upto about 74 of the axial chord from the leading edge and thereafter rose very rapidly. The incidence is found to have an effect on the passage vortex and the loss cores due to the inlet boundary layer.

NOTATION

C	: Velocity
$\overline{C}$	: Mass averaged velocity
PS	: Pressure Surface
SS	: Suction Surface
$P_{01}(z)$	: Spanwise total pressure at far upstream
$P_0(z,y)$	: Total pressure at the measurement location
e	: Blade axial chord
h	: Blade height
i	: incidence
s	: Blade pitch
x	: Distance along the axial direction
y	: Distance in pitchwise direction
z	: Distance in spanwise direction
ΔP_0	: Total pressure loss $(P_{01}(z) - P_0(z,y))$
γ	: Blade stagger angle
ζ	: Total pressure loss coefficient $\left(\frac{\Delta P_0}{0.5 \rho C_2^2}\right)$
β_{b1}	: Inlet blade angle
β_{b2}	: Exit blade angle
β_1	: Inlet flow angle
$\Delta\beta$	: Overturning/underturning angle

$\overline{\zeta}$	: Mass averaged total pressure loss coefficient

$$\frac{\int_0^{h/2} \int_0^s \zeta \rho C_{2m} \, dz \, dy}{\int_0^{h/2} \int_0^s \rho C_{2m} \, dz \, dy}$$

Subscript

1	: upstream of leading edge
2	: downstream of leading edge

INTRODUCTION

The flow in a turbomachine is quite complex and understanding of these three dimensional flows leads to improved designs with higher efficiency and better performance. The aerodynamic design of a turbine is usually carried out for its operation at design point. However, most often the turbines are also required to operate at conditions away from the design point. As a result, the inlet flow is often directed at other than the design incidence, leading to additional losses. The methods of predicting the incidence losses in a turbine are usually based on empirical correlations like Ainley and Mathieson (1951), modified later by Dunham (1970), Dunham and Came (1970) and Came(1973). The correlation technique is useful as a first order tool in turbomachinery design. However, this approach provides little insight into the nature of the secondary losses.

In the recent past, Hodson and Dominy (1987 a,b) reported the increase of secondary loss in a high speed linear cascade with increase in incidence. The production of secondary loss was observed to be greater for the positive angles of incidence. Warren and Tran (1987) showed that by decreasing the inlet flow angle at the tip region of the rotating blade and reducing the flow deflection at the hub region, it was possible to reduce the incidence and secondary flow losses. Yamamoto and Nouse (1988) discussed the effects of incidence on cascade three dimensional flows and the associated loss generation mechanism.

It can be summerised from the available information in the literature that the overall performance is affected by the presence of secondary flows and the attention is directed towards the understanding of the loss mechanism as well as the methods for reducing these losses to enhance the output from the machine leading to improved designs. The effect of incidence on the development and generation of secondary flows is one

of the parameters identified in the reviews of Sieverding (1985) and Hirayama (1987). Most of the investigations hitherto have been carried out at low Mach numbers (¡0.30). In the present investigations, the effect of variation of incidence on the generation, development and growth of secondary losses in a linear turbine cascade at an exit Mach number of 0.43 was studied by Venkata Ramana Murty (1993) for a better understanding of the secondary flows.

EXPERIMENTAL APPARATUS

The present experimental investigations were carried out on a Variable Density Cascade Tunnel (Venkata Ramana Murty, 1993), shown in Fig. 1, operating in closed circuit at the Turbomachinery Laboratory, Bharat Heavy Electricals Limited, Hyderabad. The blades for the test cascade were made of carbon steel using spark erosion method. The cascade consisted of 8 blades with an inlet angle of 139^0 and an exit blade angle of 26^0 set at a stagger angle of 72^0 with respect to tangential direction to give a geometric deflection of 113^0. The machined blades having a chord of 100 mm were assembled in the cascade box such that the space chord ratio was 0.68 and the aspect ratio was 1.52. Suitable slots were machined on the right hand side window looking from the trailing edge end corresponding to the middle passage formed by 4th and 5th blades at distances from the leading edge of 5%, 40%, and 74% of axial chord for traversing the probe within the blade passage. Slots were also machined at stations -15% axial chord upstream of the leading edge and 115% axial chord downstream of the leading edge of the cascade for detailed traversing of flow condition outside the blade passage. The traversing stations are marked as S1 to S5 in Fig. 2.
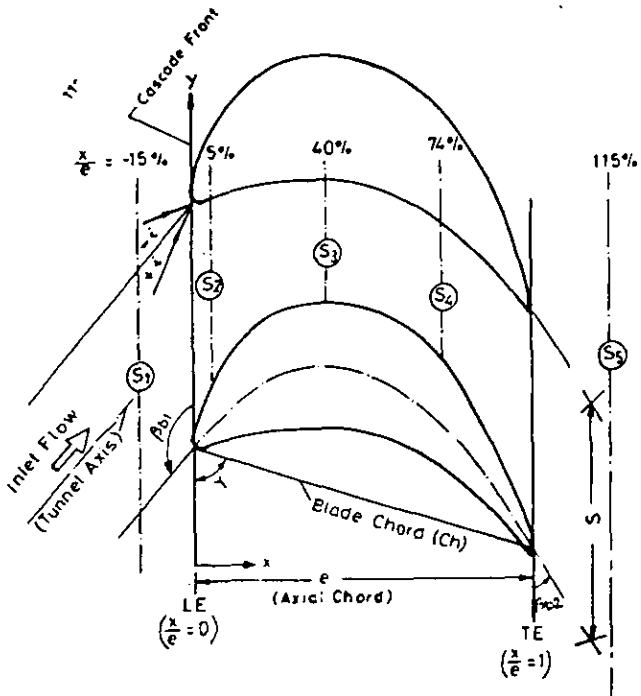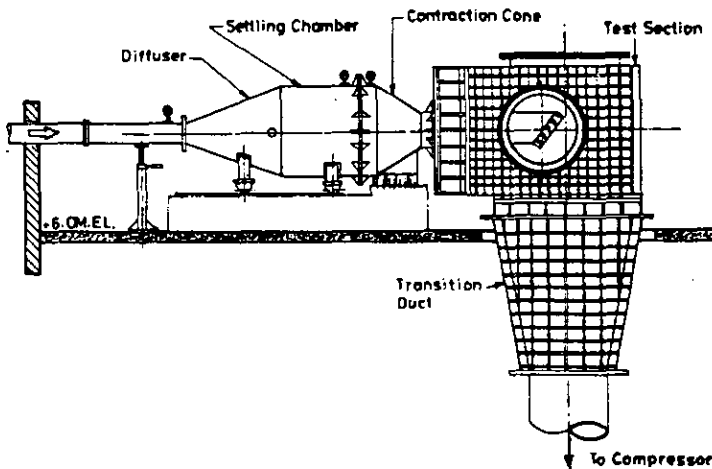

Fig 2.   LOCATION OF MEASURING STATIONS

Fig. 1. LAYOUT OF VARIABLE DENSITY CASCADE TUNNEL

A five hole hemispherical probe with a head diameter of 3.0 mm was traversed at all the five traverse stations, S1 to S5, from upstream to downstream of the cascade. The probe was traversed along the spanwise direction from the side wall to a distance a little greater than the midspan section ($z/h =$ 0.57) and in the pitchwise direction covering a little more than one blade pitch at stations S1 and S5 and for interblade flow surveys at stations S2, S3 and S4 between the suction surface and pressure surface, in order to determine the flow field within and along the blade passage. At each measuring location, the probe was nulled to make the pressures sensed by the yaw holes equal. The yaw angle and the pressure sensed by the five hole probe are recorded and the three components of velocity are determined using the calibartion chart of the probe. The probe was traversed in the spanwise direction using a semi automatic traversing mechanism.

RESULTS AND DISCUSSION

The total pressure (p_{01}) along the spanwise direction at the upstream of the cascade was measured at $x/e = -100\%$ (one chord upstream of the blade leading edge) for all the cases of incidence. The measured total pressure was normalised with the midspan total pressure $(p_{01ms})_{ms}$ and its variation along the span is shown in Fig. 3. The flow was observed to be uniform at inlet with constant total pressure over 60% of the blade span and near the endwalls the total pressure diminished as a result of the growth of the boundary layer. The total pressure profiles were observed to be similar for the range of incidence angles tested without any upstream effects of the cascade leading edge.

The effect of variation of incidence on the generation, growth and distribution of secondary flow in a linear turbine cascade is presented in the form of contours of total pressure loss coefficient at different traverse stations from S1 to S5. The investigations were carried out for 5 angles of incidence in the range $+15^0$ to -8.5^0. The variations of mass averaged total pressure loss coefficient from inlet to exit of the cascade for different angles of incidence are presented and the effect of incidence is discussed.

Contours of Total Pressure Loss Coefficient

The iso-contours of total pressure loss coefficient (ζ) computed from the total pressure at the measurement location and the total pressure at the corresponding spanwise location at one axial chord far upstream ($x/e = -100\%$) are plotted in Figs. 4 to 8 for the five cases of incidence, $i = +15^0, +5^0, 0^0, -5^0$ and -8.5^0. Although detailed flow surveys were made at 5 axial stations S1 to S5 of Fig. 2, for the sake of brevity, only three stations were chosen for the purpose of illustration viz.

$x/e = -15\%, 74\%$ and 115%. The iso-contours represent the variation of total pressure loss coefficient in the pitchwise and spanwise directions at the selected axial stations from inlet to outlet of the cascade.

Figs. 4a to 4c show the variation of total pressure loss coefficient from the inlet station S1 to the exit station S5 for the maximum positive incidence angle of 15^0.These figures show a continuous increase in the total pressure loss coefficient from

inlet to exit of the cascade in the regions close to the endwalls, corresponding to $z/h = 0.05$ to 0.30 indicating the growth of loss coefficient. The loss coefficient which was around 0.14 near the end wall at $x/e = 40\%$ was observed to decrease towards $x/e = 74\%$ and subsequently increase towards the exit station $x/e = 115\%$ and the reduction could be due to the thinning down of the incoming endwall boundary layer under the influence of the transverse pressure gradient.

The inlet boundary layer is thus seen to be discontinued and a new boundary layer developed at the maximum turning plane, $x/e \simeq 40\%$ (station S3, results not shown here), as was observed by Ye da-jun et al (1985). The new endwall boundary layer is expected to be thinner than the inlet because of the accelerating flow within the cascade passages and hence the total pressure prevailing locally in the new boundary layer can be higher than at the inlet. Gregory Smith and Graves (1983) stated that the inlet boundary layer was swept towards the suction surface at about 38% of axial chord from leading edge in a 110^0 deflection turbine cascade of aspect ratio 1.77. Such thinning down of endwall boundary layer within the cascade passage was reported by Senoo (1958), Langston et al (1977), Sieverding and Wilputte (1981), Dixon and Cooke (1982), and Gregory-Smith and Graves (1983). The total pressure loss coefficients were observed to increase sharply at the trailing end of the cascade, Fig. 4c. The contours at this station are characterised with the formation of passage vortex (marked 'PV' in Fig. 4c) with the peak values of loss coefficient occurring at the centre of the vortex. The passage vortex occupied a large area in the span and pitchwise directions and is positioned away from the blade surfaces, but a little closer to the suction surface.

The peak values of total pressure loss coefficient are seen to be moving towards the midspan and the centres of the vortices are closer to the midspan as was observed by Hodson and Dominy (1987b). The downwash of the fluid is greater on the suction surface at positive incidence and hence the centres of the passage vortices are closer to the midspan. The variation of total pressure loss coefficient from inlet to exit of the cascade for an angle of incidence of $+5^0$ is shown in Figs. 5a to 5c. Contours with large values of total pressure loss coefficient near the endwall were observed, Fig. 5a, representing the suction side and pressure side leg of the horse shoe vortex generated near the leading edge at the inlet endwall region. These vortices were observed to move towards suction surface and pressure surface respectively, Fig. 5b and 5c.
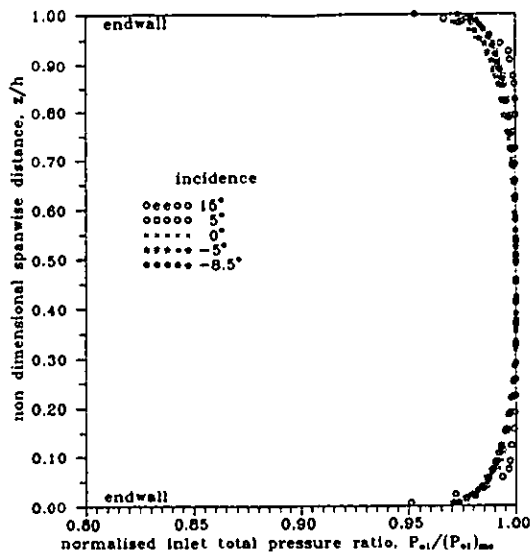

Fig. 3   Inlet Total Pressure Profiles

The passage vortex near the suction surface at $x/e = 115\%$, Fig. 5c, was observed to be placed with its centre at around $z/h = 0.20$ with large values of total pressure loss coefficient. The loss region near the pressure surface was thinner compared to that at the suction surface. The thinning of the endwall boundary layer beyond $x/e = 40\%$ and a subsequent increase of the loss coefficient in the endwall at exit were observed as was the case for $i = +15^0$. The peak value of the loss coefficient was seen more or less at the centre of the passage vortex near the suction surface. A weak formation of corner vortex with loss values of around 0.14 were noticed near the suction surface endwall corner at $x/e = 115\%$. The local loss coefficients were found to increase gradually from inlet to exit, $x/e = -15\%$ to 115%, indicating growth of losses along the cascade due to the secondary flow motions and the interaction of the endwall boundary layer with the vortex generated at the leading edge. The boundary layer growth on the suction surface appears to be considerable.
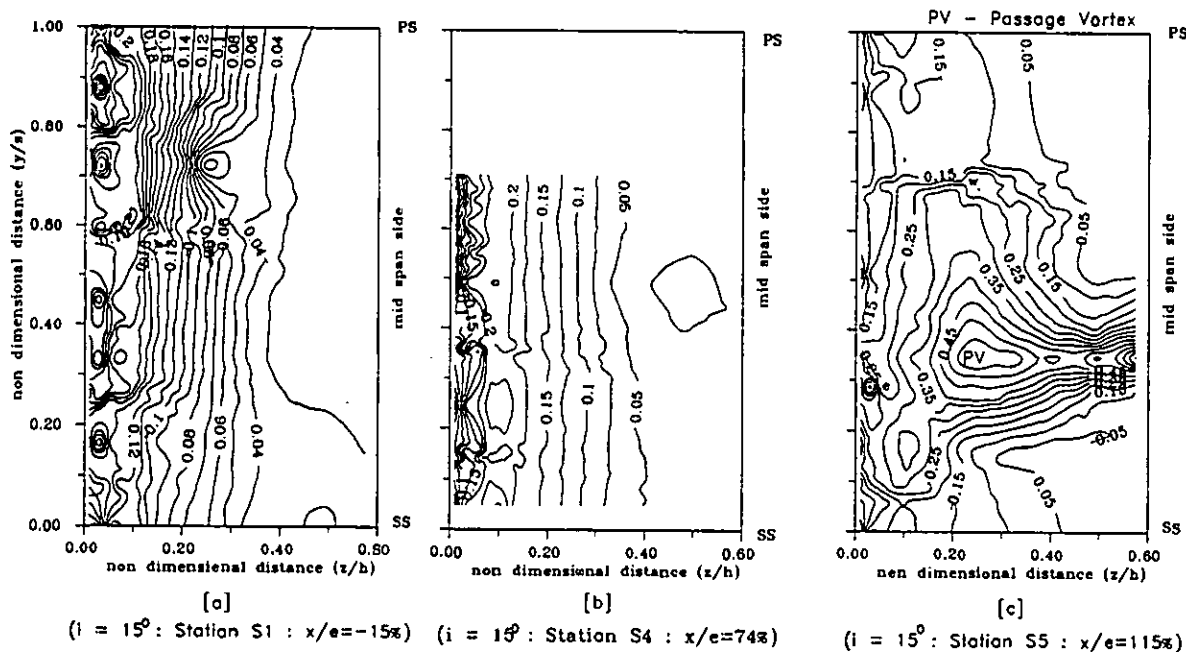

[a]
(i = 15^0 : Station S1 : x/e=−15%)   (i = 15^0 : Station S4 : x/e=74%)   (i = 15^0 : Station S5 : x/e=115%)

Fig.4   Contours of Total Pressure Loss Coefficient

3

Fig:5   Contours of Total Pressure Loss Coefficient

[a]
(i = 5°: Station S1 : x/e=−15%)

[b]
(i = 5°: Station S4 : x/e=74%)

[c]
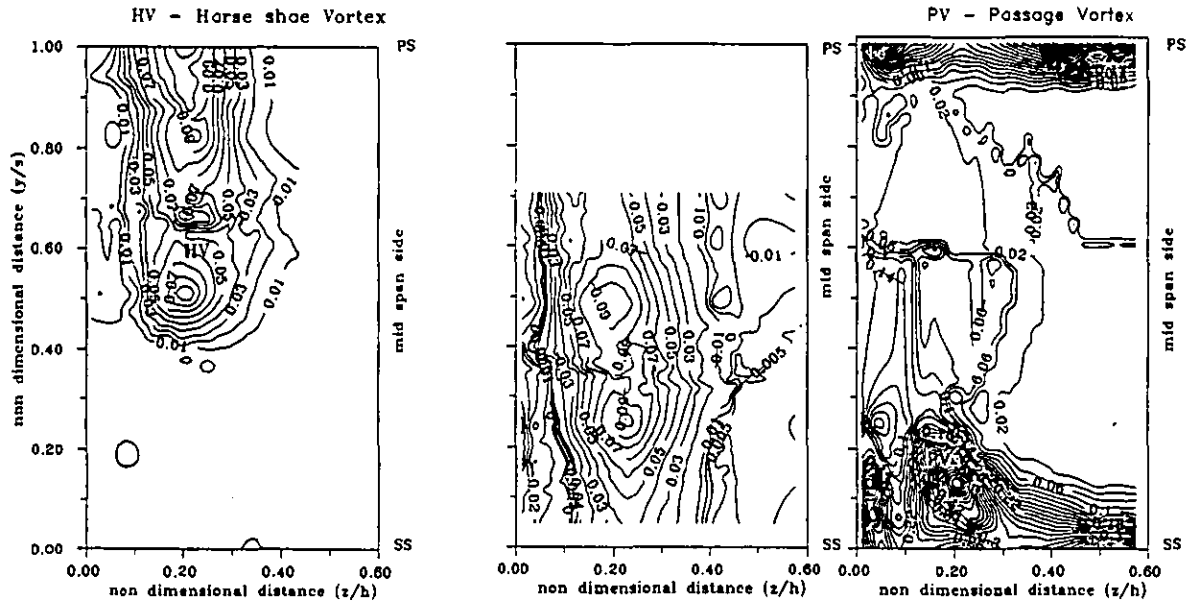(i = 5°: Station S5 : x/e=115%)
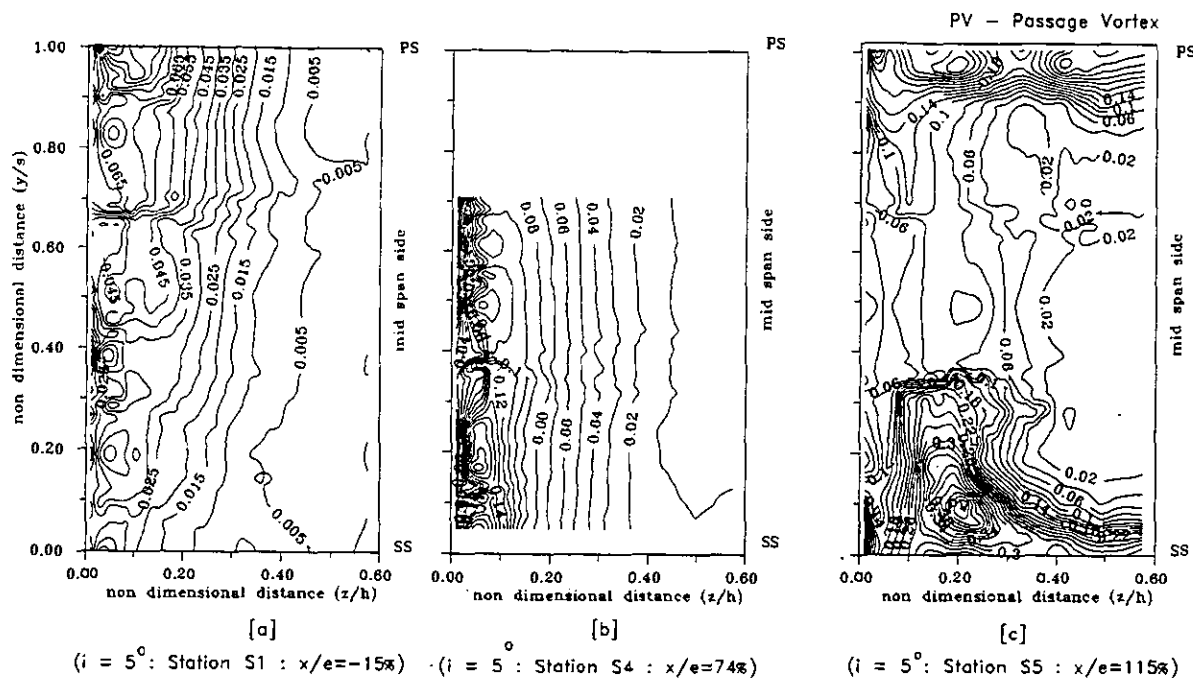
Figs. 6a to 6c show the variation of total pressure loss coefficient contours from inlet to exit of the cascade for an incidence angle of 0^0. The values of the total pressure loss coefficient increased indicating the continuous growth of losses from cascade inlet to exit. At the cascade inlet, at $x/e = -15\%$, two vortices with large values of total pressure loss coefficient were distinctly seen indicating the formation of the leading edge horseshoe vortex. The peak values of the total pressure loss coefficient were located at the centres of these vortices. Both these vortices were observed to be located at the same spanwise position. As the flow passes through the cascade, at $x/e = 5\%$, (figure not shown here), one vortex located at $z/h = 0.20$ and $y/s = 0.40$, was noticed in the measurement plane. Due to the physical constraints of the probe movements, the measurements could be taken only from $y/s = 0.3$ to 0.9 from suction surface. The vortex observed in this plane could be the pressure side leg of the horseshoe vortex moving towards the suction surface. The spanwise position has also shifted from $z/h = 0.20$ to about 0.25 indicating the secondary flow motions in the spanwise direction. This is further corroborated by the increase in the values of the total pressure loss coefficients from station 1 $x/e = -15\%$ to station 2, $x/e = 5\%$ even in the midspan region.

The passage vortex formed due to the leading edge horse shoe vortex and the endwall boundary layer was observed at stations, $x/e = 5\%$ and 40% , at $y/s = 0.40$ and $z/h = 0.20$ with large values of total pressure loss coefficient. Near the endwall at $x/e = 40\%$ and 74% , the total pressure loss coefficient was observed to be less than that at the previous station due to the thinning down of the endwall boundary layer. The passage vortex is formed by engulfing the inlet endwall boundary layer and the total pressure loss coefficient increases within the passage vortex . At the exit of the cascade at $x/e = 115\%$, the formation of the passage vortex is completed with its core centered at around $y/s = 0.10$ and $z/h = 0.20$. The peak value of the loss coefficient is seen to be located at the centre of the vortex. The large values of loss coefficients are due to the combined effect of low energy material transfer from the endwall to the blade suction side corner and the interaction of this flow with the main flow over the blade. The loss coefficients within the blade boundary layer at the pressure surface were observed to be smaller compared to the suction surface boundary layer in the midspan region.

The contours of the total pressure loss coefficient for the negative incidence of -5^0 are given in Fig. 7a to 7c at 3 axial stations along the cascade passage from inlet to exit. The trend of low values of loss near the suction surface and high values near the pressure surface were noticed at all stations from inlet to exit. The loss coefficient in the endwall boundary layer increased in the region from $x/e = -15\%$ to $x/e = 40\%$ and subsequently it got decreased with a rise at the exit station as was the behaviour of the loss coefficient at other positive angles of incidence including 0^0. These loss coefficients are relatively smaller than what were observed at 0^0 incidence. The vortex formation seen near the pressure surface could be a part of the leading edge horseshoe vortex at inlet, $x/e = -15\%$. Another region of higher loss coefficient is observed at $y/s = 0.65$ and $z/h = 0.20$. This could be a part of the suction side leg of the horseshoe vortex. Spanwise movement of the vortex from endwall towards midspan was observed.

At the exit of the cascade, $x/e = 115\%$, the existence of the passage vortex near the suction surface corner with peak loss values of around 0.44 at the centre of the vortex is noticed. The size of the vortex is not significant compared to its size at the other positive incidences. The growth of boundary layer was seen to be larger at the pressure surface compared to the suction surface as can be seen from Fig.7c. The thickness of the boundary layer was also considerable. This larger increase in losses at the pressure surface can be attributed to the flow separation from the blade leading edge which becomes one of the main cascade losses as was stated by Yamamoto and Nouse (1988). The strength of the passage vortex identified by the size of the vortex is observed to be smaller for the negative incidence angles as seen from the present investigations and was also as stated by Hodson and Dominy (1987b).

The effects of further change of the incidence were studied by conducting the experiments at $i = -8.5^0$ and the results are plotted in Figs. 8a to 8c. The leading edge horse shoe vortex was located at $y/s = 0.70$ and $z/h = 0.25$ with large values of total pressure loss coefficient. The loss contours appear to be disturbed and are not parallel to the end wall. The vortex was seen to migrate towards the pressure surface with a corresponding increase in the values of total pressure loss coefficient. The migration of the loss core was noticed only in the pitchwise direction and the location remained the same as that at

4

HV - Horse shoe Vortex

PV - Passage Vortex

[a]
(i = 0 : Station S1 : x/e = -15%)

[b]
(i = 0° : Station S4 : x/e=74 %)

[c]
(i = 0°: Station S5 : x/e = 115%)

Fig.6 Contours of Total Pressure Loss Coefficient

the inlet in the spanwise direction. A peak value of the loss coefficient of about 0.10 is observed at the centre of the vortex at $x/e = 74\%$ near the pressure surface. The magnitude of the loss coefficient increased generally in the passage between the pressure and suction surfaces near the end wall region spanning upto $z/h = 0.35$. At the exit of the cascade at $x/e = 115\%$, there is a thick blade surface boundary layer growth on the suction surface with loss coefficients of the order of 0.25. The vortex with peak loss values of around 0.45 was seen to be located at the pressure surface at z/h around 0.15 - 0.20. The fluid experiences less turning in the case of negative incidences and hence the secondary flows are reduced and so the transverse pressure gradients may not be substantial. This may be one of the reasons for the vortex to lie near the endwall region as was observed by Vijayaraghavan (1987) at -7^0 incidence.

Mass Averaged Loss Parameters

The local total pressure loss coefficients deduced at different measuring stations are averaged both in the pitchwise and spanwise directions to obtain the overall mass averaged total pressure loss coefficient $(\overline{\zeta})$, the net secondary loss coefficient $(\overline{\zeta_s})$ and the profile (midspan) loss coefficient for all the angles of incidence investigated and are plotted in Fig. 9. It is seen from the figure that the total pressure loss coefficient increased with increase or decrease in incidence on either side of the zero incidence. The rate of increase was observed to be more for positive incidence compared to the negative incidence showing up an asymmetry in the variation. This is mainly due to the local separation on the suction surface at positive incidences

PV - Passage Vortex

[a]
(i = -5 : Station S1 : x/e=-15 %)

[b]
(i = -5 : Station S4 : x/e=74 %)
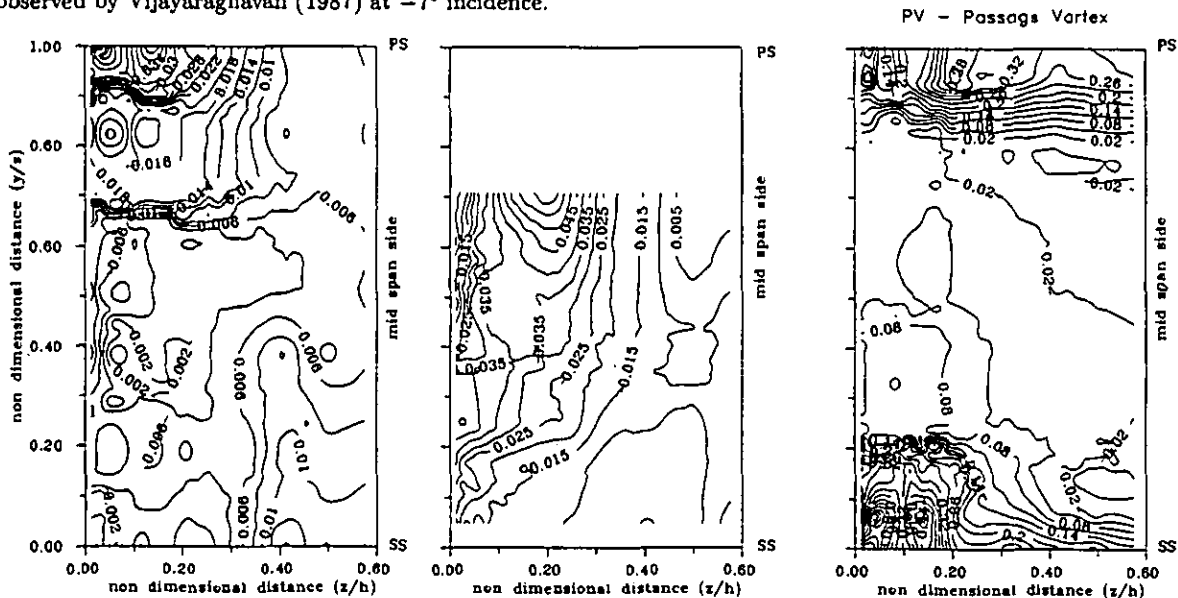
[c]
(i = -5 : Station S5 : x/e=115 %)

Fig. 7   Contours of Total Pressure Loss Coefficient

5

[a]
(i = −8.5 : station S1: x/e = −15%)

[b]
(i = −8.5 : Station S4 : x/e = 74%)

[c]
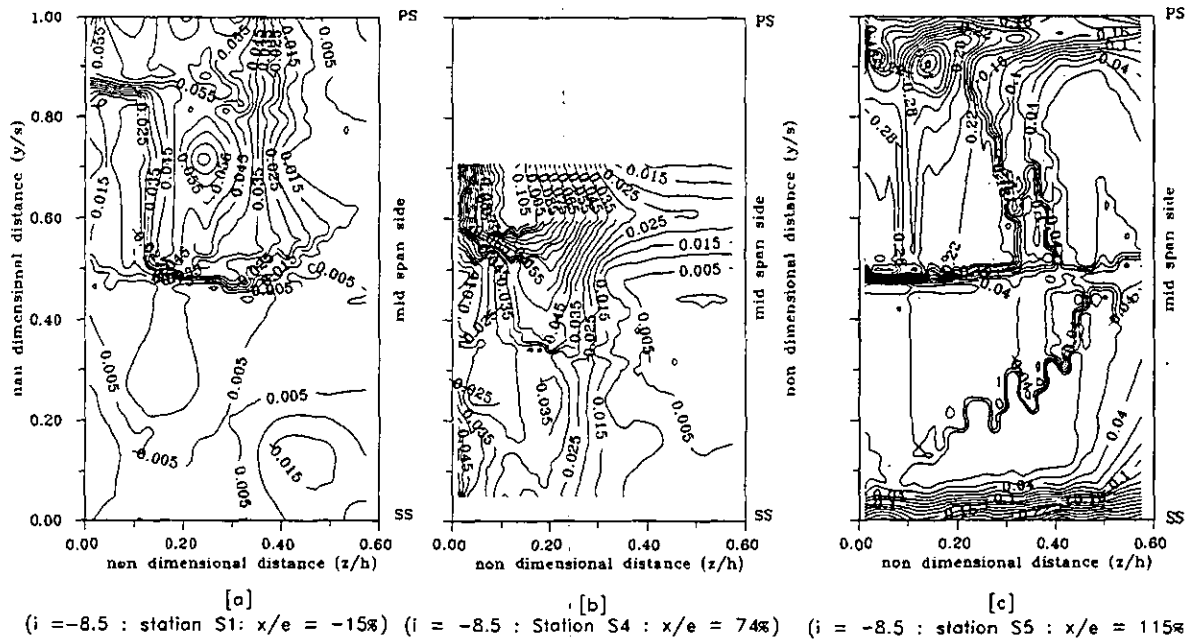(i = −8.5 : station S5 : x/e = 115%)

Fig. 8 Contours of Total Pressure Loss Coefficient

compared to the smaller area of separation at corresponding values of incidence in the negative direction. The secondary loss was observed to be increasing steeply towards the positive incidence compared to the negative angles of incidence. The fluid experiences less turning at the negative angles of incidence as it passes through the cascade and hence experiences reduced secondary flows. In the present investigations, for this cascade, it can be mentioned from the figure that it is the secondary loss coefficient which is playing a predominant role in increasing the overall total pressure loss coefficient for the positive angles of incidence.

Fig. 10 shows the variation of mass averaged total pressure loss coefficient ($\bar{\zeta}$) averaged in pitchwise and spanwise directions at each axial measuring station of the cascade. The variation of the total pressure loss coefficient was found to be the highest for the maximum positive angle of incidence in the present studies ie. $+15^0$. Yet another observation from this figure is that with increasing angles of incidence in the positive direction, the averaged total pressure loss coefficient is generally found increasing from inlet Station, $x/e = -15\%$ to exit station, $x/e = 115\%$. The rate of increase is observed to be more near the trailing edge region commencing from $x/e = 74\%$. The total pressure losses at the trailing edge region increase due to the contributions made by the midspan losses and wake losses. The present experimental data shows that the rapid rise in the total pressure loss coefficient occurs downstream of the passage starting from $x/e = 74\%$. The growth may be attributed to the interaction of the endwall cross flow with the suction side boundary layer. The rolling up of the low energy fluids on to the suction surface might be commencing from $x/e = 74\%$ in the present studies causing a steep rise in the secondary loss.

The variation of the net secondary loss coefficient ($\bar{\zeta}_s$) averaged in spanwise and pitchwise directions is shown in Fig. 11. The figure reveals that the net secondary loss coefficient increases with the increased incidence. It is also observed that the rate of growth of secondary loss is steady after entering the cascade and shoots up near the trailing edge plane. Larger turning of the flow in the cascade produces higher losses near the endwalls and near the blade surfaces. These increased losses lead to an increase in the overall loss coefficient for positive angles of incidence. Moreover, the migration of low energy fluid from the endwall increases with increase in incidence and hence, the secondary loss coefficient increased with increase in incidence. It is observed that after a slight increase near the

leading edge plane, the net secondary loss coefficient remains constant upto 74% of axial chord behind leading edge and then increases rapidly beyond this position towards trailing edge for angles of incidence $i = +15^0, -5^0$ and -8.5^0. The rate of increase for 0^0 and $+5^0$ was not all that rapid as was the case with other incidences, although there is an increase in the net secondary loss coefficient.

It is seen from the above discussions on the evolution and growth of the total pressure loss coefficient and secondary loss coefficient that the losses grow steadily from inlet to about $x/e = 74\%$ and then rises rapidly towards the trailing edge. This is in line with the observations of Sieverding and Wilputte (1981), Marchal and Sieverding (1977) and Gregory-Smith et al (1988).
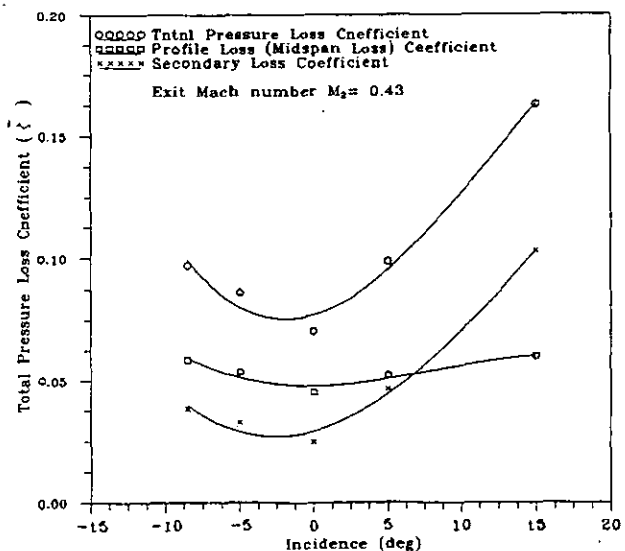

Fig. 9   Variation of Mass Averaged Total Pressure Loss Coefficient (Station S5 : x/e=115%)
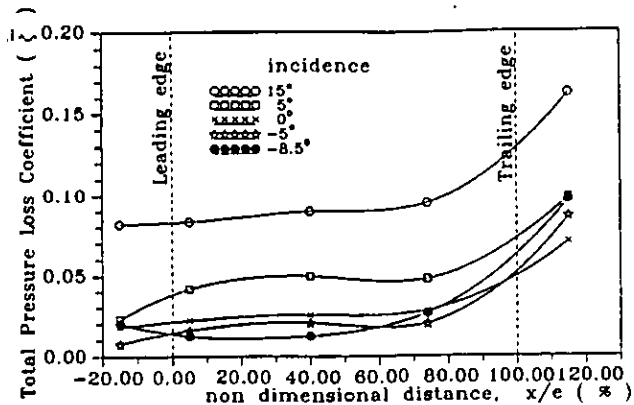
Fig. 10 Variation of Total Pressure Loss Coefficient along the Cascade

There are two main features of a turbine cascade secondary flow, the passage vortex and the loss core associated with the inlet boundary layer. The passage vortex convects the loss core across the passage to the suction surface. These features can be studied in a comprehensive manner at the exit of the cascade. Hence the variation of total pressure loss coefficient at $x/c = 115\%$ for all the angles of incidence investigated is shown in Fig. 12. These curves show the dependence of the loss coefficient on the angle at which the cascade receives the flow or the angle of incidence. The largest values of loss coefficients are observed for the positive incidence of $+15^0$ in the present studies. The peak loss coefficient was observed to decrease with decrease in incidence upto 0^0 and then again rise as the incidence is further decreased in the negative direction. The midspan flows seem to be affected only at the extreme angles of incidence investigated namely $+15^0$ and -8.5^0.

The passage vortex becomes stronger with increased turning through the cascade and it can show up its influence right upto the midspan as is noticed in the present studies. Otherwise the loss shown at the midspan represents the 2-D profile loss which is observed over 60% of the full span assuming that the conditions are symmetric in the other half of the unexplored distance of the span. At all other values of angles of incidence the endwall secondary flow effects are felt upto $z/h = 0.30$ to 0.35. The position of the peak value of loss coefficient is seen to be at $z/h = 0.15$ for $-8.5^0, 5^0$, and 0^0 whereas it has moved to $z/h = 0.20$ for $+5^0$ incidence and to 0.25 at $+15^0$ incidence. As stated earlier the movement of the loss peak towards midspan depends on the strength of the passage vortex. The variation of the pitch averaged loss coefficient, in general, depends on the position of the passage vortex which in turn depends on the inlet wall boundary layer thickness, aspect ratio and blade loading (Vijayaraghavan, 1987). Since the loss peak has moved considerably at $+15^0$ incidence, it seems that the passage vortex is stronger at the maximum positive incidence. Yamamoto and Nouse(1988) observed that the passage vortex generated in the cascade is very strong at $+7.2^0$.
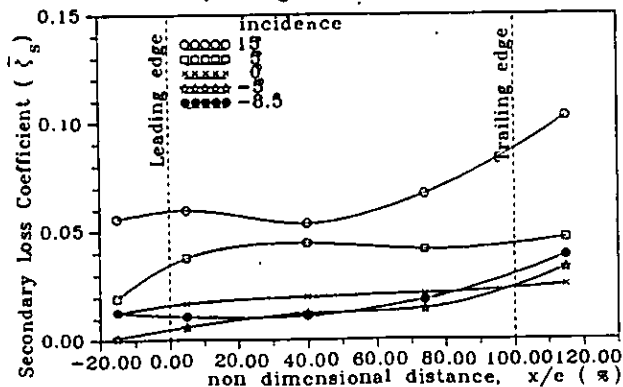

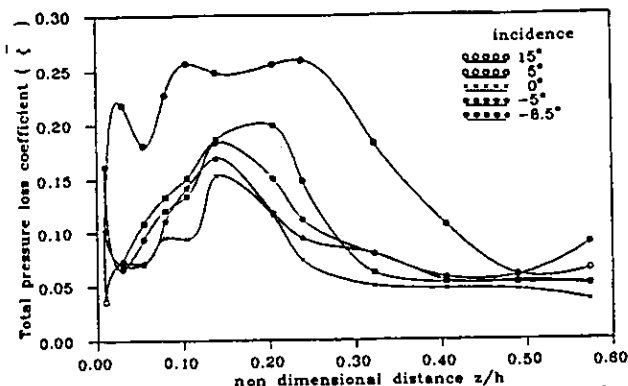**Fig. 11 Variation of Secondary Loss Coefficient along the Cascade**

Fig. 12 Spanwise Variation of Pitchwise averaged Total Pressure Loss Coefficient (Station S5 : x/c=115 %

Apart from the passage vortex becoming stronger at higher positive incidence values, it can also be viewed that the suction surface boundary layer is turbulent over much of its length and hence the midspan loss increases at positive incidences (Hodson and Dominy, 1987b). The double loss peak distribution is observed at $i = 0^0$ and at $i = +15^0$. Mobarak et al (1989) showed that the high loss zones appear near the endwall at the trailing edge and lie near the suction surface and the endwalls, at $i = 0^0$ and $M_2 = 0.4$. They also stated that the aspect ratio and the turning angle of the rectilinear cascade affect the positions of the secondary flow pattern. The turning angle is related to the incidence and the present experimental investigations confirm such a dependence of the generation and growth of secondary flows on the incidence.

Only a single loss peak is noticed in the present studies at $i = +5_0$ and -5^0. Came (1973) gave a likely explanation that the secondary loss is primarily due to the boundary layer swept by the passage secondary flow, but the high trailing velocities will draw in this fluid of low stagnation pressure and cause the concentration of the losses into a single peak. Two peaks are observed when the passage secondary vorticity is of comparable magnitude to the trailing vortices, then the vortices of opposite senses cause two concentrations of the low stagnation fluid resulting in two loss peaks. The separation at the negative incidence and the intensity of the passage vortex becoming stronger at the positive incidence seem to be the main reasons for the spanwise flows causing secondary flows in a blade cascade extending upto midspan region at the exit of the cascade. It may be summed up that the main factor leading to the development of the cascade secondary flow is the existence of shear flow near the endwall of the cascade inlet region.

Variation of Momentum Averaged Flow Angle

The secondary flow causes the flow angle to deviate from the primary flow angle which will have an adverse effect on the work transfer in the subsequent stages in a multi stage turrbine. The effects of the variation of the momentum averaged outlet flow angle with incidence in the spanwise direction is shown in Fig. 13 in the form of overturning/ underturning angle $(\Delta\bar{\beta})$. The flow is overturned near the endwall and underturned away from the endwall and near the the midspan. The overturning near the wall is seen to be maximum at around $z/h = 0.05$ and the position of maximum overturning remained the same for almost all the angles of incidence. The amount of overturning was found to be maximum for $i = +15^0$.

A general trend of underturning near the midspan and overturning near the endwall was noticed for $i = +5^0, 0^0$ and -5^0 whereas the flow remained mostly overturned for the extreme angles of positive and negative incidence. The outlet flow angle is controlled by the magnitude and location of the passage vortex. The overturning of the flow near the endwall indicates that the flow tries to migrate more strongly towards the suction surface and this effect increases with increase in incidence. As the incidence changes, the loading distribution changes on the blade surface and these changes in the flow conditions seem to alter the overturning near the wall.
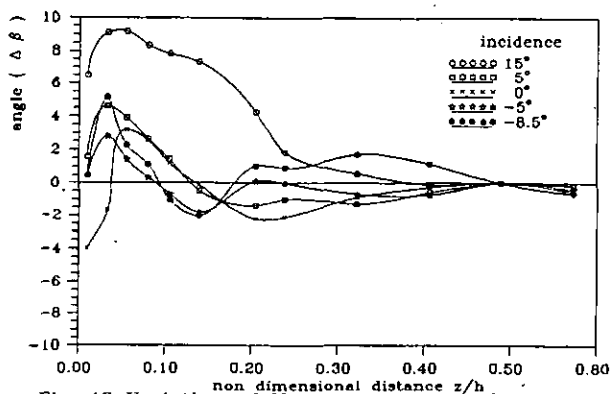
7

Fig. 13 Variation of Momentum averaged Flow Angle
(x/e ≈ 115%)

The overturning at 0^0 and -5^0 near the endwall appear to be small whereas the underturning is maximum at 0^0 incidence occurring at $z/h = 0.20$. The flow has been continuously overturning at $i = 15^0$ upto the midspan. Very close to the endwall, the overturning is seen to be getting reduced. This may be due to the effects of corner vortex near the suction surface/endwall corner on the flow turning. These corner vortices may be caused by the endwall shear stresses and they draw back the overturning flows in the underturning direction. Sieverding (1985) indicated that the presence of corner vortex near the endwall can be identified by the characteristic reduction of the overturning near the endwall in the spanwise distribution of flow angle.

Blade Surface Pressure Distribution

The surface static pressures on the suction and pressure surface of the instrumented blade of the cascade were measured at three spanwise positions $z/h = 0.066$, 0.133 and 0.50 for angles of incidence $i = 5, 0^0$ and -5^0 to study the effect of incidence on the blade loading due to the development of secondary flows. Fig.14 shows the blade loading at $i = 5^0$ at different spanwise positions. It is observed that the spanwise position has no significant effect on the pressure distribution as was observed by Adjlout and Dixon, 1992. The region of separation on the suction surface was noticed between $x/e = 30\%$ and 50% whereas the mass averaged total pressure loss coefficient showed a steep rise at $x/e = 74\%$.
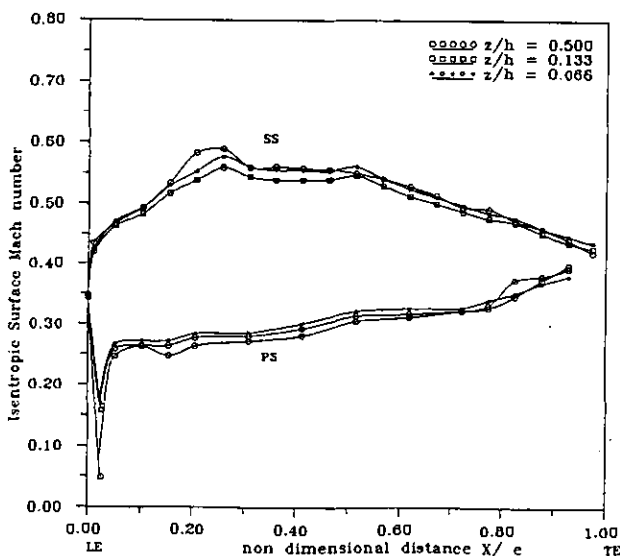

Fig. 14 Surface Mach Number Distribution
(incidence i = +5)

CONCLUSIONS

The contours of the total pressure loss coefficient and the mass averaged results in the pitch and spanwise directions gave a more meaningful information on the development and growth of the secondary flows in a linear turbine cascade. The two main features of the turbine cascade secondary flow namely the passage vortex and the loss cores associated with the inlet boundary layer were observed in a comprehensive manner at the exit of the cascade in the present investigations. The passage vortex seen at the downstream plane is the strongest at the maximum positive angle of incidence. With decrease in incidence, it gets weaker and the amount of low energy fluid on the suction side decreases rapidly. The evolution and development of the total pressure loss coefficient indicated the growth of these losses steadily from cascade inlet upto an axial distance of 74% and then rise rapidly towards the trailing edge. The outlet flow angle is seen to be controlled by the location and magnitude of the passage vortex. The characteristic reduction in the overturning near the endwall indicated the presence of corner vortices.

REFERENCES

Adjlout, L. and Dixon, S.L., 1992, "Endwall losses and FlowUnsteadiness in a Turbine Blade cascade," ASME Journal of Turbomachinery, Vol.114, pp.191-197.

Ainley, D.G. and Mathieson, G.C.R., 1951, "A Method of Performance Estimation for Axial Flow Turbines," ARC R&M 2974.

Came,P.M., 1973, "Secondary Loss Measurements in a Cascade of Turbine Blades," Institution of Mechanical Engineers Conf. Publication 3, pp 75-83.

Dunham, J., 1970, "A Review of Cascade data on Secondary Losses in Turbines," Jl. of Mech. Engg. Sciences, Vol. 12, No. 1, pp 48 - 59..

Dunham, J. and Came, P.M., 1970, "Improvements to the Ainley-Mathieson Method of Performance Prediction," Trans. ASME, 52A, 252.

Gregory-Smith, D.G. and Graves, C.P., 1983, "Secondary Flows and Losses in a Turbine Cascade," AGARD Conf. Proceedings No.351 on Viscous Effects in Turbomachinery, Copenhagen, Denmark.

Gregory-Smith D.G., Graves, C.P. and Walsh, J.A., 1988, "Growth of Secondary Losses and Vorticity in an Axial Turbine Cascade," ASME Journal of Turbomachinery, Vol. 110, PP. 1 - 8.

Hirayama, N., 1987, "Recent Research on the Flow Through Turbine Blade Rows," JSME International Journal, Vol. 30, No. 269, pp. 1699-1706.

Hodson, H.P. and Dominy, R.G., 1987a, "Three-Dimensional Flow in a Low Pressure Turbine Cascade at its Design Condition," ASME Journal of Turbomachinery, Vol. 109, pp. 177 - 185.

Hodson, H.P. and Dominy, R.G., 1987b, "The Off-Design Performance of a Low-Pressure Turbine Cascade," ASME Journal of Turbomachinery, Vol. 109, pp.201 - 209.

Langston, L.S., Nice, M.L. and Hooper R.M., 1977, "Three Dimensional Flow within a Turbine Cascade Passage," ASME Journal of Engg. for Power, pp. 21 - 28.

Marchal Ph. and Sieverding, C.H., 1977, "Secondary Flows within the Turbomachinery Blading," AGARD Conf. Proc. No. 214 on Secondary Flows, The Hague, The Netherlands.

Mobarak, A., Khalafallah, M.G., Heikal, H.A. and Osman, M.A., 1989, "Study of Various Factors Affecting Secondary Loss Vortices Downstream a Stright Turbine Cascade," ASME Paper, 89-GT-12.

Senoo, Y., 1958, "The Boundary layer in the Endwall of a Turbine Nozzle Cascade," Tr. ASME, Vol. 80, pp. 1711.

Sieverding, C.H., and Wilputte, Ph., 1981, "Influence of Mach Number and EndWall Cooling on Secondary Flows in a Straight Nozzle Cascade," ASME Journal of Engg. for Power, Vol. 103, pp. 257 - 264.

Sieverding, C.H., 1985, "Recent Progress in the Understanding of Basic Aspects of Secondary Flows in Turbine Blade Passages," ASME *Journal of Engg. for Gas Turbines and Power*, Vol. 107, No.2, pp 248 - 257.

Venkata Ramana Murty, G., 1993, "Secondary Flow Studies in a Rectangular Bend and in a Linear Turbine Cascade," Ph.D. Thesis, IIT, Madras.

Vijayaraghavan, S.B., 1987, "Effects of Free Stream Turbulence, Reynolds Number and Incidence Angle on Axial Turbine Cascade Performance," Ph.D. Thesis, Iowa State University, Ames, Iowa.

Warren, R.E. and Tran. M.H., 1987, "Recent Developments to improve High-pressure and Intermediate-pressure Turbine Efficiency," Proceedings of Instn.of Mech. Engineers, International Conference, 1-3 Sept., Robinson College, Cambridge, Paper No. C 278/87.

Yamamoto, A and Nouse, H., 1988, "Effects of Incidence on Three-Dimensional Flows in a Linear Turbine Cascade," ASME Paper No. 88-GT-110.

Ye Da-Jun, Zhou Li-wei., 1985, "Experimental Research of the Secondary Flow in Rectilinear Turbine Cascade," *Journal of Chinese Engineering Thermophysics*, 2.

9